

Supplementary Information

for

Photophysical, electrochemical and anion sensing properties of Ru(II) bipyridine complexes with 2, 2'-biimidazole-like ligands

Hao-Jun Mo, Yan-Li Niu, Mei Zhang and Zheng-Ping Qiao Bao-Hui Ye*

MOE Key Laboratory of Bioinorganic and Synthetic Chemistry, School of Chemistry and Chemical Engineering, Sun Yat-Sen University, Guangzhou 510275, China. E-mail: cesybh@mail.sysu.edu.cn.

Measurement Methods

Elemental (C, H, and N) analyses were performed on an Elementar Vario EL analyzer. Electrospray ionization mass spectra (ESI-MS) were obtained on a Thermo LCQ DECA XP mass spectrometer. ¹H NMR spectra were obtained on a Varian Mercury-Plus 300 spectrometer. Electronic absorption spectra were obtained with a Shimadzu UV-3150 spectrophotometer. Emission spectra were recorded on a Hitachi F-4500 fluorescence spectrometer. Electrochemical measurements were carried out with a CHI-630C electrochemistry system. pH measurements were performed with a Mettler Toledo S20P pH meter equipped with an InLab Science Pro electrode. NMR, UV, luminescence spectra and electrochemical properties were recorded at 298 K.

pKa Determination: A 50 cm³ solution consisted of 40 % acetonitrile, 60 % water, 0.1 mol·dm⁻³ phosphoric acid, and 6×10⁻⁵ mol·dm⁻³ **3** was prepared in a 25 °C titration vessel, magnetic stirring was employed during the whole experiment. 1 mol·dm⁻³ NaOH aqueous solution was added dropwise into the vessel, after each addition, pH value and absorption spectra of the mixed solution were recorded. The *pKa* value was fitted from the equation below:¹

$$pK_a = pH - \log \frac{A - A_{HA}}{A_{A^-} - A}$$

where *A*_{HA}, *A*_{A⁻}, and *A* refer to the absorbances at the initial, final, and intermediate pH values at a given wavelength.

UV and Luminescence Titration: Quartz cuvettes with a 1 cm path length and a 3 cm³ volume were used for all measurements. For a typical titration experiment, 3 μL aliquots of tetrabutylammonium (TBA)

salts of F⁻, OAc⁻, Cl⁻, Br⁻, I⁻, NO₃⁻, and HSO₄⁻ (0.005 mol·dm⁻³ in acetonitrile) were added to a 2.5 cm³ solution of **3** (6×10⁻⁵ mol·dm⁻³ in acetonitrile). For luminescence titration, the excitation wavelength was 470 nm, the excitation slit width was maintained at 5 nm, and the emission slit width at 10 nm.

Quantum yields were determined in freeze-thaw-pump degassed solutions of the complexes by a relative method using [Ru(bpy)₃]²⁺ in the same solvent as the standard.² The quantum yields were calculated by the equation below:³

$$\Phi_r = \Phi_{\text{std}} \frac{A_{\text{std}} I_r \eta_r^2}{A_r I_{\text{std}} \eta_{\text{std}}^2}$$

where Φ_r and Φ_{std} are the quantum yields of unknown and standard samples ($\Phi_{\text{std}} = 0.062$,⁴ 298 K, in acetonitrile at $\lambda_{\text{ex}} = 450$ nm), A_r and A_{std} are the solution absorbance at the excitation wavelength (λ_{ex}), I_r and I_{std} are the integrated emission intensities, and η_r and η_{std} are the reflective indices of the solvent. Experimental errors in the reported luminescence quantum yields were about 20 %.

¹H NMR Titration: 1.25 μL aliquots of TBA salts of F⁻, OAc⁻, Cl⁻, Br⁻, I⁻, NO₃⁻, and HSO₄⁻ (0.12 mol·dm⁻³ in acetonitrile-*d*3) were added to a 400 μL solution of **1**, **2** and **3** (0.003 mol·dm⁻³ in acetonitrile-*d*3). Titration of **3** with F⁻, OAc⁻ and OH⁻ was also performed in DMSO-*d*6 solutions. Spectra were recorded after each addition, and the sample shaken thoroughly before each measurement.

Electrochemical measurements in acetonitrile: A three-electrode assembly comprising of a glassy carbon working electrode, a Pt auxiliary electrode, and a non-aqueous Ag/AgNO₃ reference electrode were used. The cyclic voltammetric (CV) and square wave voltammetric (SWV) measurements were carried out in acetonitrile solution of the complex (0.001 mol·dm⁻³) and the concentration of the supporting electrolyte (TBAPF₆) was maintained at 0.1 mol·dm⁻³. Nitrogen was bubbled into the solution for 10 min and the glassy carbon electrode was polished with an alumina / water slurry before each measurement. A scan rate of 100 mV·s⁻¹ was employed for all measurements. The potentials obtained in acetonitrile were referenced against the Ag/AgNO₃ electrode, which under the given experimental conditions gave a value of 0.07 V for the Fc/Fc⁺ couple. The $E_{1/2}$ values were determined from CV using the relation $E_{1/2} = 0.5(E_{\text{pc}} + E_{\text{pa}})$, where E_{pc} and E_{pa} were cathodic and anodic potentials, respectively, and also directly obtained from the peak values of SWV curves.

The diagram of Ru^{2+/3+} potential vs pH: A three-electrode assembly comprising of a glassy carbon working electrode, a Pt auxiliary electrode, and an aqueous Ag/AgCl reference electrode were used. The

$\text{Ru}^{2+/3+}$ potentials were obtained from SWV measurements, which were carried out in acetonitrile / water (2:3 / V:V) solution of **3** ($0.001 \text{ mol}\cdot\text{dm}^{-3}$). Different buffer systems (0.1 mol dm^{-3}) were employed over different pH ranges: 0 – 2, perchlorate; 2 – 4, phthalate; 4 – 8, phosphate; 8 – 12, borate.⁵ The potentials obtained in acetonitrile / water were referenced against the Ag/AgCl electrode, which under the given experimental conditions gave a value of 0.26 V for the Fc/Fc⁺ couple (remained constant over the pH range 0 – 12).

Table S1 Photophysical and Redox Properties of **1**, **2**, **3** and $[\text{Ru}(\text{bpy})_3]^{2+}$ in acetonitrile at 298 K

	Abs, $\lambda_{\text{max}} / \text{nm}$ ($10^{-4} \epsilon / \text{M}^{-1} \text{cm}^{-1}$)	Lum. $\lambda_{\text{max}} / \text{nm}$	Φ_{r}^a	Oxid. b / V	Red. b / V
1	290 (4.98), 341 (0.84), 475 (0.80)	638 ^c	4.5×10^{-3}	0.71	-1.86, -2.14, -2.24
2	290 (4.94), 330 (3.10), 348 (3.53), 465 (0.96)	624 ^c	2.8×10^{-3}	0.73	-1.82, -2.08, -2.19
3	290 (5.01), 332 (3.35), 349 (3.54), 462 (1.08)	617 ^c	2.8×10^{-3}	0.74	-1.80, -2.06, -2.18
$[\text{Ru}(\text{bpy})_3]^{2+}$	287 (5.03), 450 (1.00)	597 ^d	6.2×10^{-2e}	0.97	-1.65, -1.84, -2.10

^a Estimated errors were about 20%. ^b vs. Ag/AgNO₃, which gives $E_{1/2} = 0.07 \text{ V}$ for Fc/Fc⁺. ^c $\lambda_{\text{ex}} = 470 \text{ nm}$. ^d $\lambda_{\text{ex}} = 450 \text{ nm}$. ^e Ref. 4

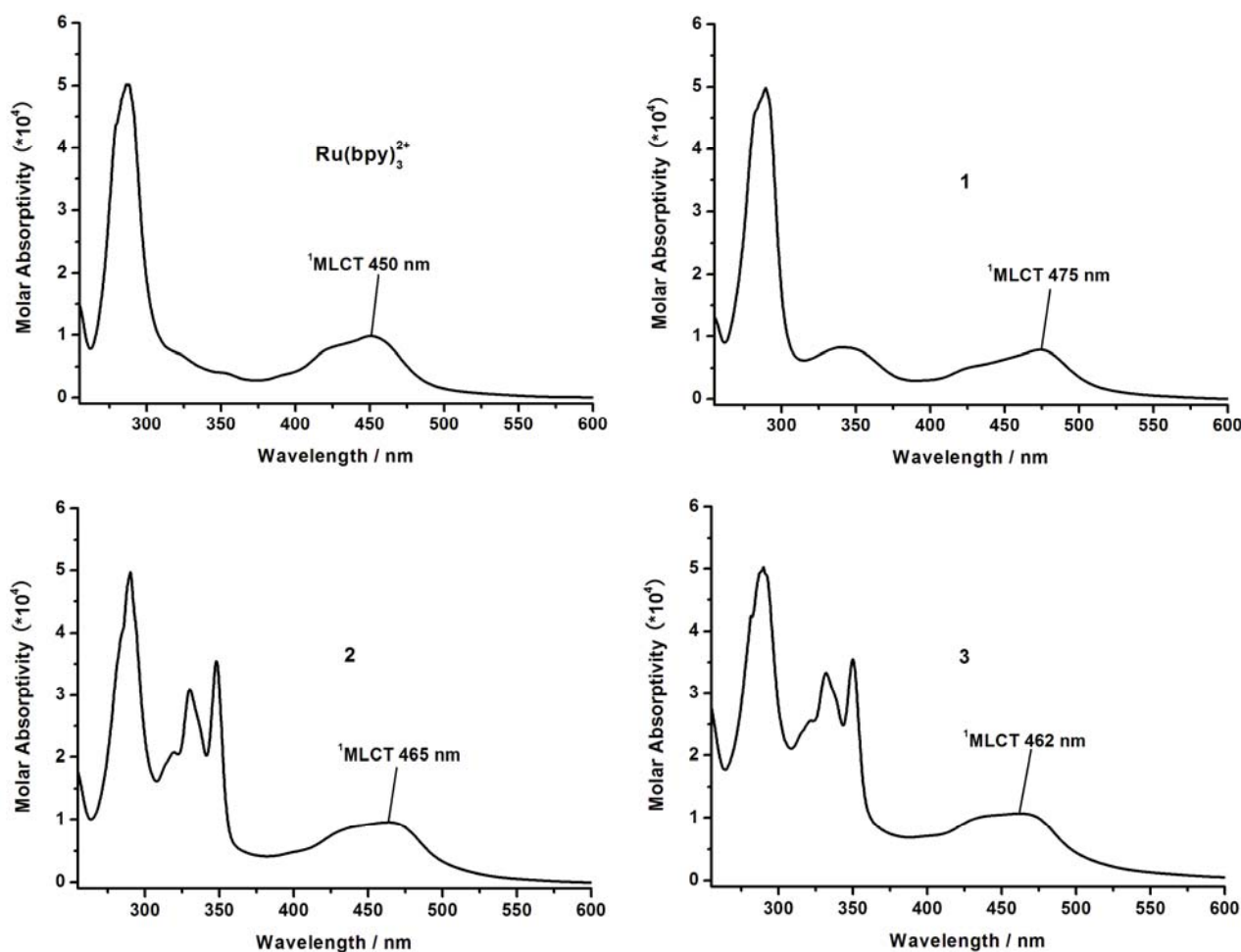


Fig. S1 Absorption spectra of $[\text{Ru}(\text{bpy})_3]^{2+}$, **1**, **2** and **3** in acetonitrile at 298 K

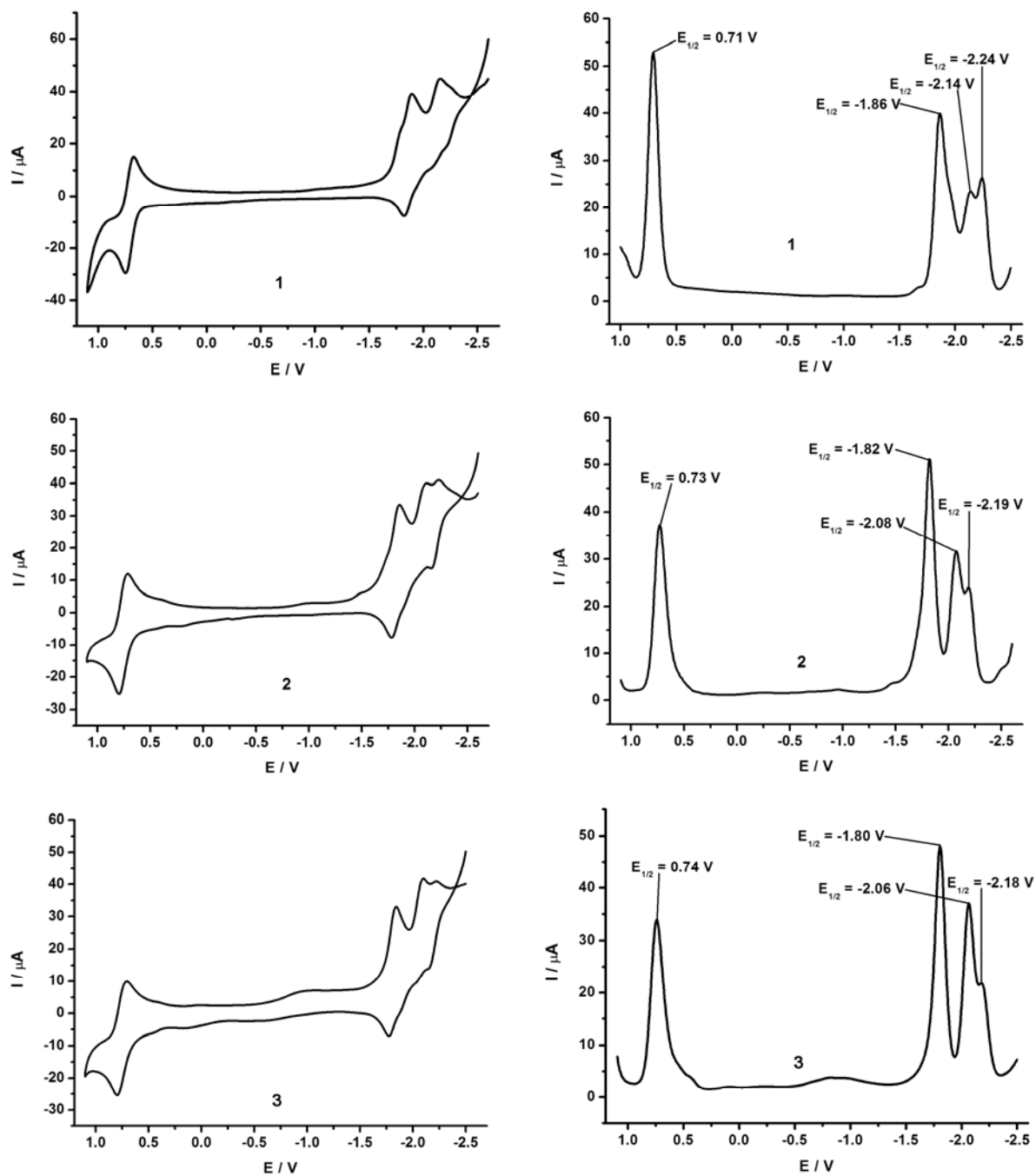


Fig. S2 CV (left) and SWV (right) curves of **1**, **2** and **3** in acetonitrile with a scan rate of $100 \text{ mV}\cdot\text{s}^{-1}$ at 298 K (vs. Ag/AgNO₃)

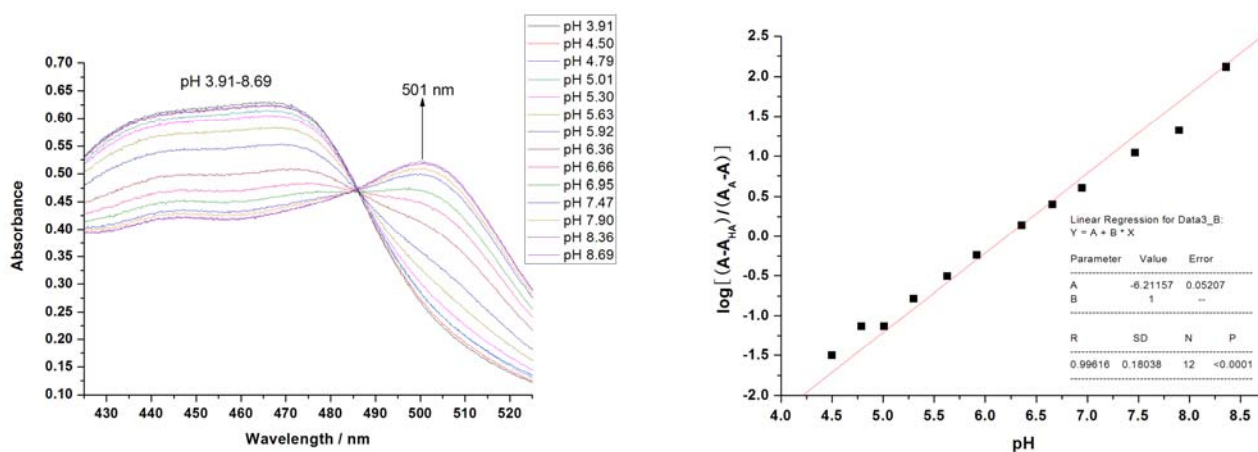


Fig. S3 Determination of pK_{a1} of **3** by UV method. Left: Absorption spectral change as pH value increases. Right: Linear fitting of pK_a value.

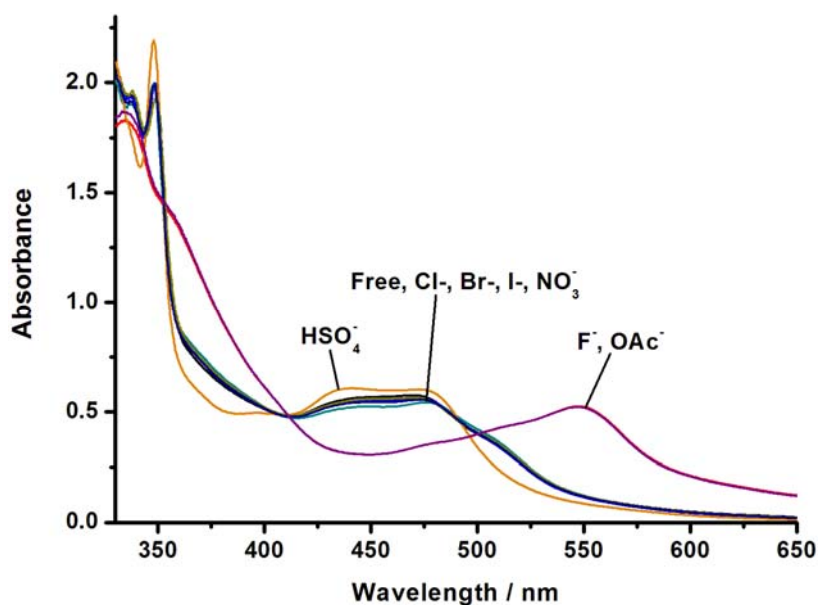


Fig. S4 Absorption spectral changes of **3** (6×10^{-5} mol·dm⁻³) in acetonitrile upon addition of 10 equiv of different anions.

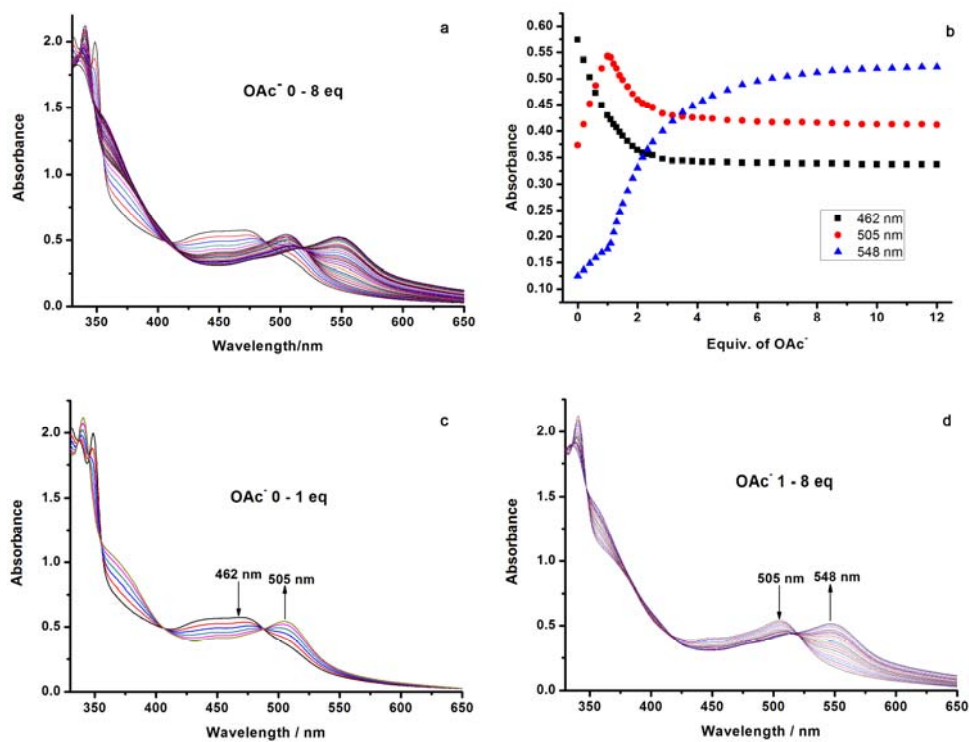


Fig. S5 UV-vis titration of **3** ($6 \times 10^{-5} \text{ mol} \cdot \text{dm}^{-3}$) in acetonitrile upon addition of OAc^- (a) 0 – 8 equiv, (c) 0 – 1 equiv, and (d) 1 – 8 equiv. (b) Absorbance at 462, 505 and 548 nm versus equivalents of OAc^- .

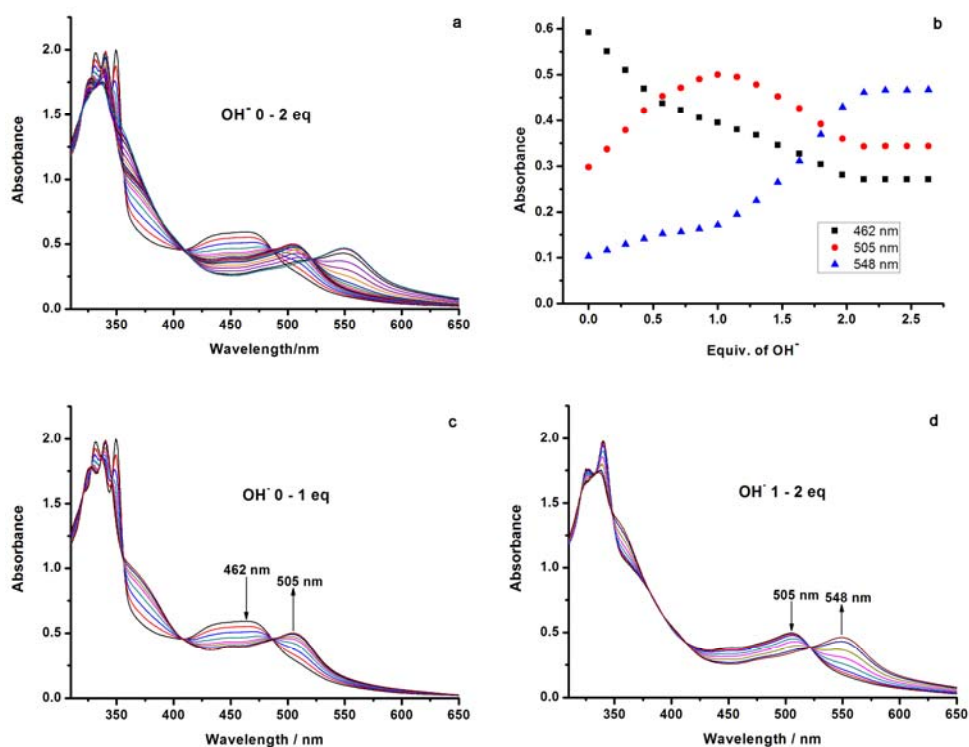


Fig. S6 UV-vis titration of **3** ($6 \times 10^{-5} \text{ mol} \cdot \text{dm}^{-3}$) in acetonitrile upon addition of OH^- (a) 0 – 2 equiv, (c) 0 – 1 equiv, and (d) 1 – 2 equiv. (b) Absorbance at 462, 505 and 548 nm versus equivalents of OH^- .

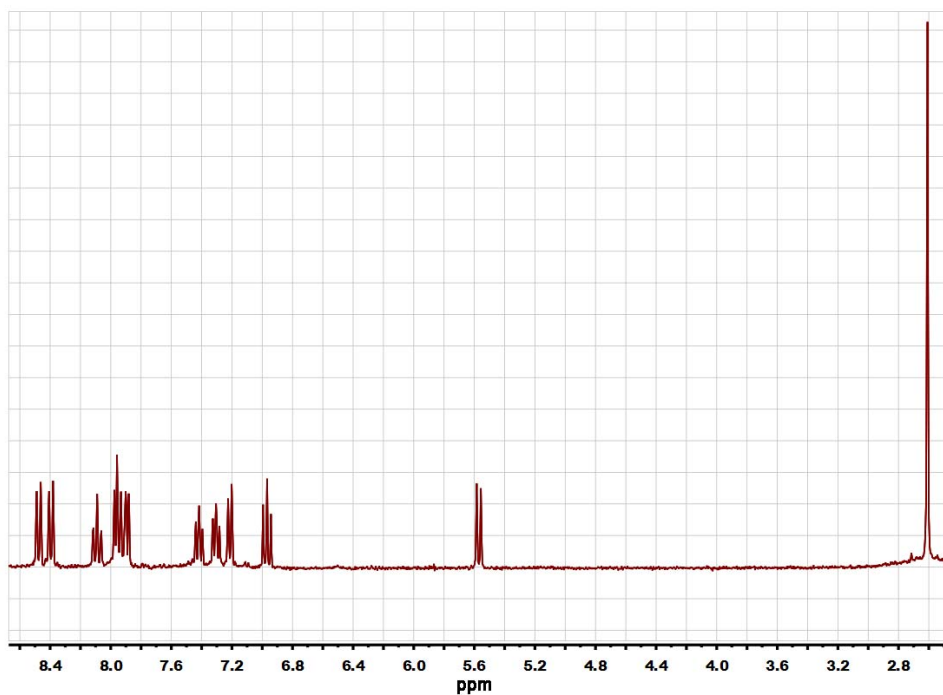


Fig. S7 ^1H NMR spectra of **3** in acetonitrile- d_3 (298K, 300 MHz).

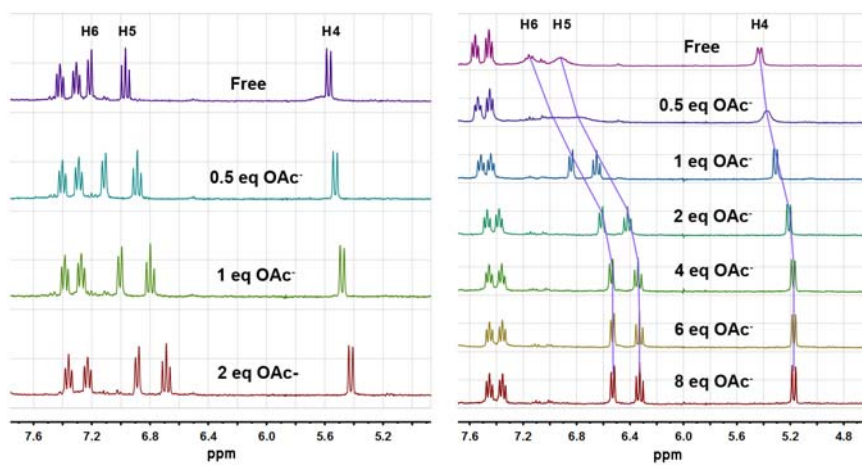


Fig. S8 ^1H NMR titration of **3** ($0.003 \text{ mol}\cdot\text{dm}^{-3}$) in acetonitrile- d_3 (left) and DMSO- d_6 (right) with OAc^- (298K, 300MHz).

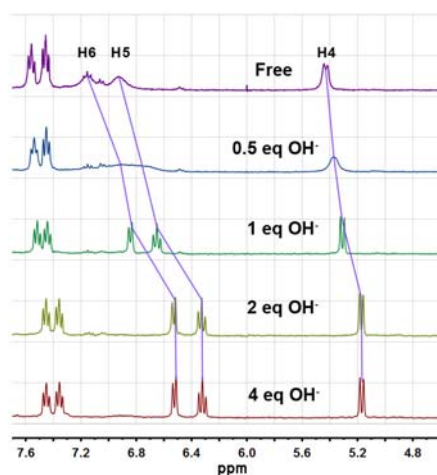


Fig. S9 ^1H NMR titration of **3** in $\text{DMSO-}d_6$ ($0.003 \text{ mol}\cdot\text{dm}^{-3}$) with OH^- (298K, 300MHz).

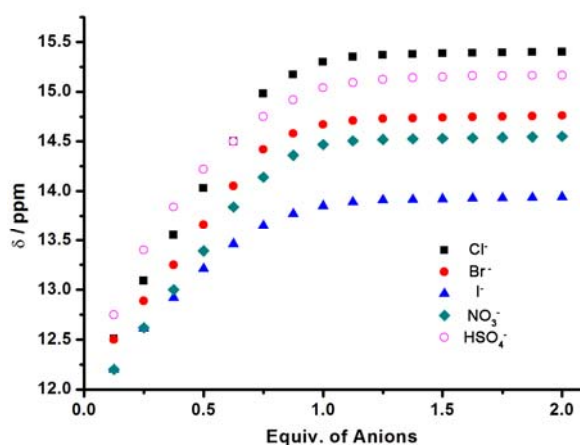


Fig. S10 Chemical shift changes of the N-H signal of **3** ($0.003 \text{ mol}\cdot\text{dm}^{-3}$ in acetonitrile- d_3) upon addition of Cl^- , Br^- , I^- , NO_3^- and HSO_4^- anions.

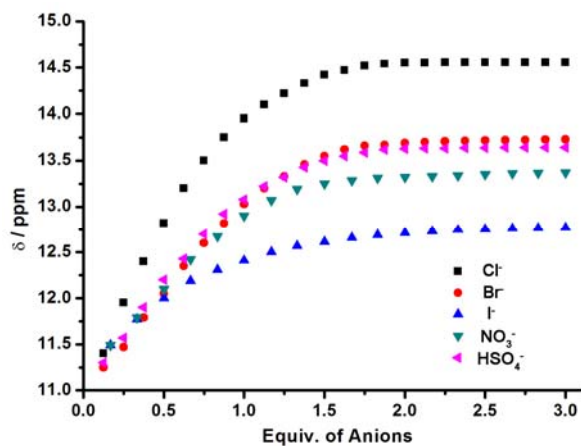


Fig. S11 Chemical shift changes of the N-H signal of **1** ($0.003 \text{ mol}\cdot\text{dm}^{-3}$ in acetonitrile- d_3) upon addition of Cl^- , Br^- , I^- , NO_3^- and HSO_4^- anions.

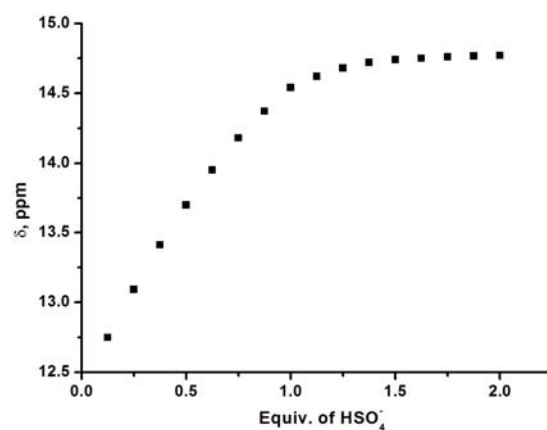


Fig. S12 Chemical shift change of the N-H signal of **2** ($0.003 \text{ mol}\cdot\text{dm}^{-3}$ in acetonitrile- d_3) upon addition of HSO_4^- .

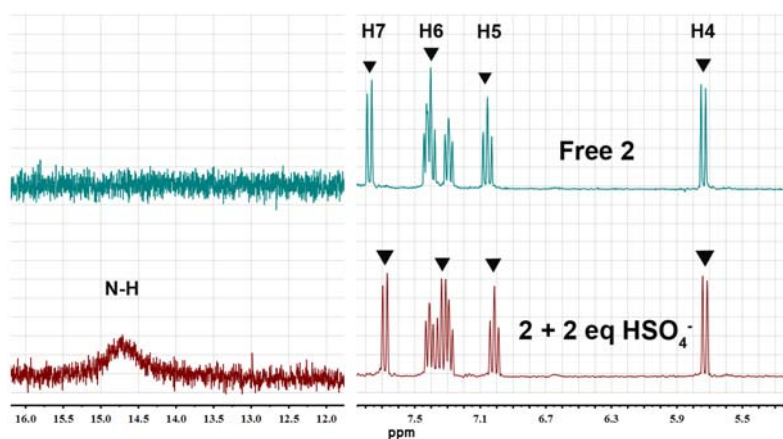


Fig. S13 ^1H NMR spectra of **2** ($0.003 \text{ mol}\cdot\text{dm}^{-3}$ in acetonitrile- d_3) in the absence and presence of 2 equiv of HSO_4^- (298 K, 300 MHz)

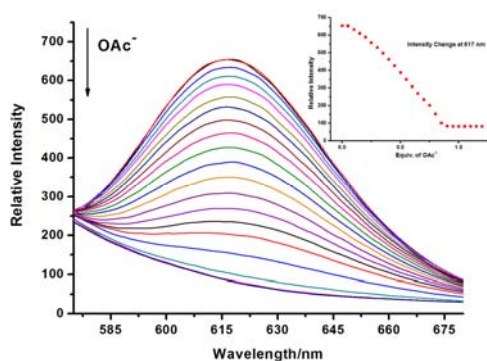


Fig. S14 Emission spectral response of **3** ($6 \times 10^{-5} \text{ mol}\cdot\text{dm}^{-3}$ in acetonitrile, 298K, $\lambda_{\text{ex}} = 470 \text{ nm}$) upon addition of OAc^- anion. Inset: Intensity at 617 nm versus equiv of OAc^- .

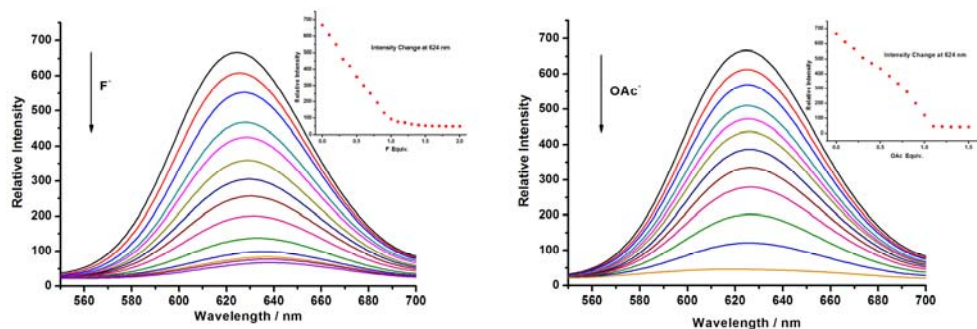


Fig. S15 Emission spectral responses of **2** (6 × 10⁻⁵ mol·dm⁻³ in acetonitrile, 298K, λ_{ex} = 470 nm) upon addition of F⁻ (left) and OAc⁻ (right). Insets: Intensity at 624 nm versus equiv of anions.

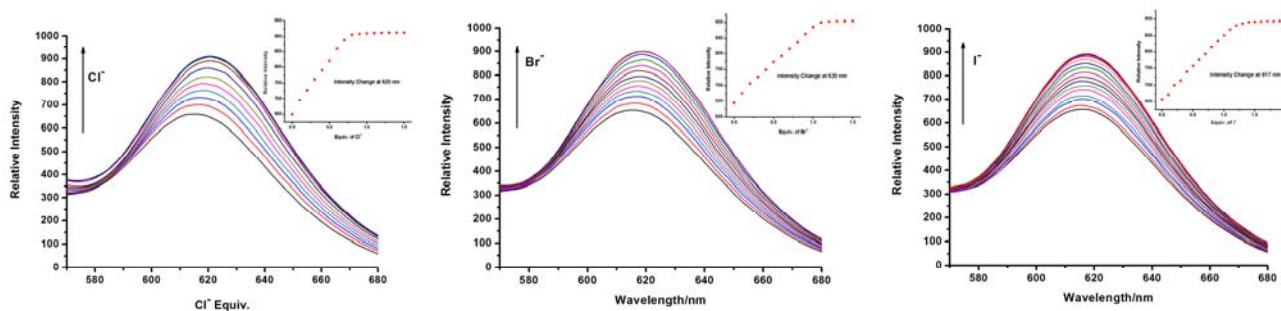


Fig. S16 Emission spectral responses of **3** (6 × 10⁻⁵ mol·dm⁻³ in acetonitrile, 298K, λ_{ex} = 470 nm) upon addition of Cl⁻, Br⁻ and I⁻ anions. Insets: Intensity at 620, 620 and 617 nm versus equiv of anions.

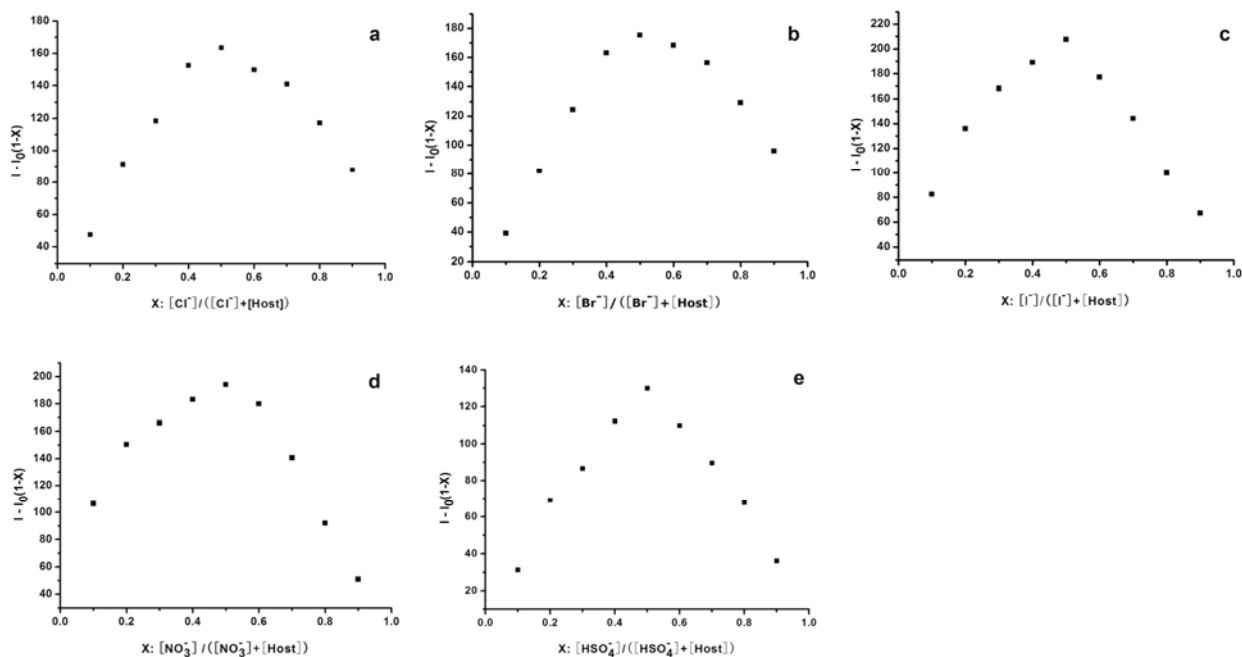


Fig. S17 Job plot analyses for **3** and (a) Cl⁻, (b) Br⁻, (c) I⁻, (d) NO₃⁻ and (e) HSO₄⁻.

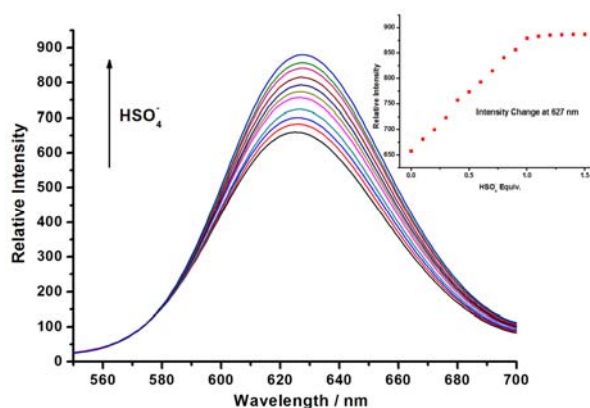


Fig. S18 Emission spectral response of **2** ($6 \times 10^{-5} \text{ mol} \cdot \text{dm}^{-3}$ in acetonitrile, 298K, $\lambda_{\text{ex}} = 470 \text{ nm}$) upon addition of HSO_4^- . Inset: Intensity at 627 nm versus equiv of HSO_4^- .

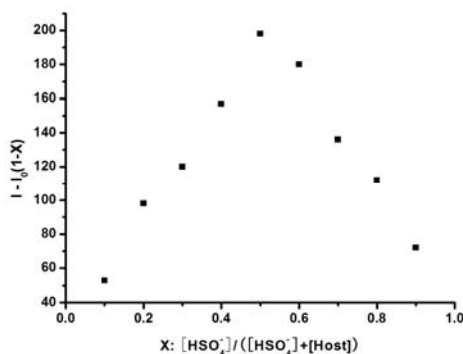


Fig. S19 Job plot analysis for **2** and HSO_4^- .

Table S2 Binding constants of **2** and **3** with 5 different anions in CH_3CN calculated from emission spectra (errors are given in parentheses) ^a

Anion	Log <i>K</i>	
	2	3
Cl^-	-	5.31 (0.05)
Br^-	-	5.24 (0.07)
I^-	-	5.21 (0.04)
NO_3^-	-	5.18 (0.04)
HSO_4^-	5.16 (0.06)	5.20 (0.05)

^a Fitted to the equation⁶
$$\Delta F = \frac{\Delta \varepsilon ([\text{H}] + [\text{G}] + \frac{1}{K}) \pm \sqrt{\Delta \varepsilon^2 ([\text{H}] + [\text{G}] + \frac{1}{K})^2 - 4 \Delta \varepsilon^2 [\text{H}][\text{G}]}}{2}$$

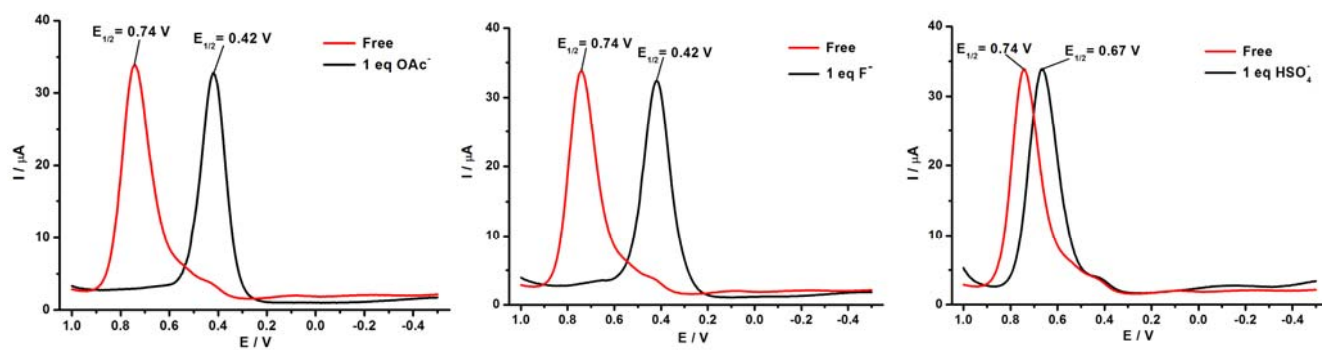


Fig. S20 SWV measurements of **3** in acetonitrile ($0.001 \text{ mol}\cdot\text{dm}^{-3}$) in the absence and presence of 1 equiv of OAc^- , F^- or HSO_4^- (vs. Ag/AgNO_3).

References

1. K. Connors, *Binding constants: the measurement of molecular complex stability*, Wiley, New York, 1987.
2. B. Sullivan, D. Salmon, T. Meyer and J. Peedin, *Inorg. Chem.*, 1979, **18**, 3369-3374.
3. J. Van Houten and R. Watts, *J. Am. Chem. Soc.*, 1976, **98**, 4853-4858.
4. J. Calvert, J. Caspar, R. Binstead, T. Westmoreland and T. Meyer, *J. Am. Chem. Soc.*, 1982, **104**, 6620-6627.
5. D. Perrin and B. Dempsey, *Buffers for pH and metal ion control*, Chapman & Hall, London, 1974.
6. Y. Liu, B.-H. Han and Y.-T. Chen, *J. Phys. Chem. B*, 2002, **106**, 4678-4687.